I&EC research
Industrial & Engineering Chemistry Research

Article

pubs.acs.org/IECR

Facile Synthesis and Acetone Sensing Performance of Hierarchical SnO_2 Hollow Microspheres with Controllable Size and Shell Thickness

Jiao Li,[†] Pinggui Tang,*[,†,‡] Jiajun Zhang,[†] Yongjun Feng,[†] Ruixian Luo,[†] Aifan Chen,[†] and Dianqing Li*[,†,‡]

[†]State Key Laboratory of Chemical Resource Engineering, and [‡]Beijing Engineering Center for Hierarchical Catalysts, Beijing University of Chemical Technology, Beijing 100029, P. R. China

Supporting Information

ABSTRACT: A facile method to prepare SnO_2 hollow microspheres has been developed by using SiO_2 microspheres as template and Na_2SnO_3 as tin resource. The obtained SnO_2 hollow microspheres were characterized by X-ray diffraction, scanning electron microscopy, high resolution and transmission electron microscopy, and Brunauer−Emmett−Teller analysis, and their sensing performance was also investigated. It was found that the diameter of SnO_2 hollow microspheres can be easily controlled in the range of 200−700 nm, and the shell thickness can be tuned from 7.65 to 30.33 nm. The sensing tests showed that SnO_2 hollow microspheres not only have high sensing response and excellent selectivity to acetone, but also exhibit low operating temperature and rapid response and recovery due to the small crystal size and thin shell structure of the hollow microspheres, which facilitate the adsorption, diffusion, and reaction of gases on the surface of SnO_2 nanoparticles. Therefore, the SnO_2 hollow microsphere is a promising material for the preparation of high-performance gas sensors.

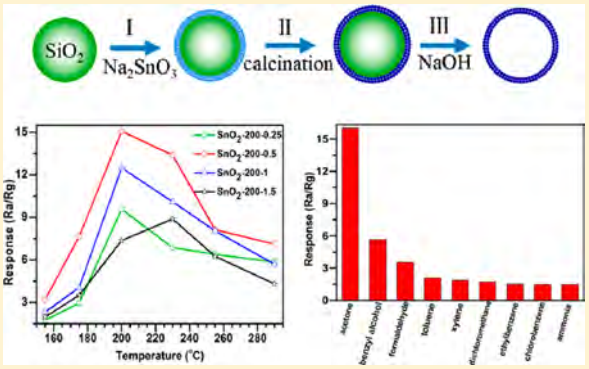

1. INTRODUCTION

Acetone, easy to combust and evaporate at room temperature, is an extensively used chemical reagent in lab and industry. It may cause many health hazards to human beings, such as headache, narcosis, and so forth, at concentrations higher than 500 ppm. Moreover, the mixture of its vapor and the air will explode when the volume concentration of acetone is in the range of 2.6−12.8%. Moreover, the concentration of acetone exhaled by I diabetic patients is higher than that of healthy people.[1] However, the current diagnosis of diabetes requires a blood test, which is not only inefficient, but also painful for patients. Therefore, the fast detection of acetone through a facial method is vitally important to ensure the health and safety of human beings.

Gas sensors, which play a pivotal role in detecting harmful and inflammable gases, have been widely used in the fields of industry, agriculture, electronics, and daily life. Because of their advantages of small size, low cost, simple operation, and good reversibility, semiconductor sensors become one of the most promising devices among the solid-state chemical sensors.[2] Many oxide semiconductors have been explored to detect pollutant, toxic, and inflammable gases, such as ZnO,[3] SnO_2,[4] TiO_2,[5] In_2O_3,[6,7] Fe_2O_3,[8] and WO_3.[9] Generally, the sensing mechanism of semiconductors relates to the surface adsorption and surface reaction of target gases on the semiconductors, which results in a reduction/oxidation process of the semiconductors. The effects of these surface phenomena are reversible and lead to the significant change in electrical resistance.[10]

Among the most studied metal oxide semiconductors, SnO_2, acting as a gas sensing materials, has attracted considerable attention for the advantages of excellent heat tolerance, corrosion resistance, low cost,[11] and good sensing response to acetone.[12,13] Chen et al.[14] reported that SnO_2 nanopolyhedrons had superior response to acetone and shorter response and recovery times at 370 °C. Qin et al.[15] investigated the gas sensitivity of square-shaped SnO_2 nanowires to acetone, and found that the sensitivity reached 5.5 at the concentration of 20 ppm at 290 °C, and the response and recovery times were 7 and 10 s, respectively. However, the shortcomings such as high working temperature, large energy consumption, and poor selectivity restrict the application of SnO_2 material in practice. Hence, the design and synthesis of SnO_2 material with low operating temperature and excellent sensing performance is more desirable in accordance with the demand in industry.

Received: January 8, 2016
Revised: March 3, 2016
Accepted: March 8, 2016
Published: March 8, 2016

DOI: 10.1021/acs.iecr.6b00060
Ind. Eng. Chem. Res. 2016, 55, 3588−3595

It has been proven that the gas sensing response increases abruptly when the particle size becomes comparable or smaller than the Debye length (typically several nanometer).[2] Nanoparticles with size in the range of several nanometers show high response to target gases. However, owing to their small particle size, nanoparticles have poor stability when they are used as gas sensing materials. Hierarchical structures assembled by low dimension building-blocks, such as 0D nanoparticles, 1D nanowires, 1D nanorods, and 2D nanosheets, and so on, not only retain the high specific surface area of low dimensional nanostructures, but also have more open mesoporous structures, which benefits the gas diffusion. Hollow spheres, a typical hierarchical structure, have attracted lots of attention because of their high specific surface area and excellent diffusion property, and hollow spherical metal oxide semiconductors show outstanding gas sensing performance.[16] For example, the sensitivity of SnO_2 hollow spheres to 100 ppm ethanol was 119 at 250 °C, which is much larger than the response of SnO_2 nanoparticles (18) at 200 °C.[17] SnO_2 hollow spheres, synthesized by heat treatment of a mixture composed of $SnCl_4$ and carbon templates, showed a sensing response of 75 to 1000 ppm ethanol at 300 °C, and very fast response and recovery times of 4 and 10 s.[18] Qian et al. reported that SnO_2 hollow spheres showed a higher response of 6.8 to 40 ppm ethanol at room temperature.[19] These results indicate that the less agglomerated configuration and open porous hollow structures enhance the gas sensitivity, shorten the response and recovery times, and reduce the operating temperature. Nevertheless, the relatively thick shell and larger crystallite size of SnO_2 hollow spheres hinder the diffusion of target gases and have an adverse effect on the sensing performance,[20] and the sensing performance of SnO_2 hollow spheres toward acetone is rarely reported. Thereby, it is desirable to prepare SnO_2 hollow microspheres with thin thickness and small crystal size, and study its sensing performance to acetone.

Herein, we report a simple method for preparation of SnO_2 hollow microspheres with controllable size and shell thickness by using SiO_2 microspheres as a template, and the influence of the structure on acetone gas sensing properties has been investigated. The obtained results reveal that SnO_2 hollow microspheres with small diameter, thin shell thickness, and small crystal size exhibited the merits of high sensing response to acetone, good sensing selectivity, fast response and recovery, and low operating temperature. Hence, this study offers guidance for optimizing the structure of gas sensing materials, and these SnO_2 hollow microspheres have potential application in industry.

2. EXPERIMENTAL SECTION

2.1. Material. Tetraethyl orthosilicate ($Si(OC_2H_5)_4$, denoted as TEOS, purity > 98%) was provided by Aladdin Industrial Co., Ltd. $Na_2SnO_3{\cdot}4H_2O$ (purity > 98%) was purchased from Sinopharm Chemical Reagent Beijing Co., Ltd. CH_3CH_2OH, $NH_3{\cdot}H_2O$, and NaOH were all of analytical grade and used without any further purification. Deionized water was used throughout the experiments.

2.2. Preparation of SnO_2 Hollow Microspheres. The preparation process of SnO_2 hollow microspheres are illustrated in Scheme 1. The monodisperse silica microspheres with different sizes were prepared by hydrolyzing tetraethyl orthosilicate in ethanol solvent in the presence of deionized water and ammonia according to the modified Stöber method.[21] Specifically, a mixed clear solution of ethanol, deionized water, and ammonia was vigorous stirred for 30 min, then TEOS was added into the mixed solution with stirring at room temperature for 4 h. The volume of ethanol and ammonia remained constant (46.60 and 6.75 mL, respectively), and the volume of TEOS and deionized water was varied to obtain SiO_2 microspheres with the desired size. Mixtures of 1.42, 1.42, and 5.68 mL of TEOS with 27, 6.45, and 6.45 mL of deionized water were used to prepare SiO_2 microspheres with mean size of 200, 500, and 700 nm, respectively. The final precipitate was washed with deionized water and ethanol for several times, and then dried at 60 °C overnight. Finally, the dried powder was annealed at 500 °C for 4 h, and SiO_2 microspheres with a mean size of 200, 500, and 700 nm were denoted as SiO_2-200, SiO_2-500, and SiO_2-700, respectively.

Scheme 1. Illustration for Fabrication of SnO_2 Hollow Microspheres

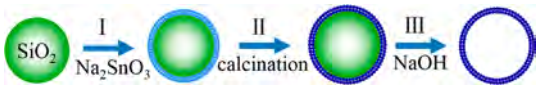

SiO_2@SnO_2 microspheres were prepared by in situ deposition method. Typically, 0.60 g of SiO_2-200 microspheres were dispersed in 50 mL of deionized water under ultrasonication for 20 min. Respective amounts of 0.71, 1.42, 2.84, and 4.27 g of $Na_2SnO_3{\cdot}4H_2O$ with Sn/Si molar ratio of 0.25, 0.5, 1, and 1.5 were dissolved in 100 mL mixed solution of deionized water and ethanol (V:V = 1:1). Then, the solution of Na_2SnO_3 was added into the suspension liquid of SiO_2 microspheres, and the mixture was magnetically stirred at 60 °C for 3 h to form SiO_2@SnO_2 microspheres. SiO_2@SnO_2 microspheres were separated by centrifugation, washed with deionized water and ethanol for several times, and then dried at 60 °C for overnight, followed by calcination at 400 °C for 4 h at a heating rate of 5 °C·min^{-1} under flowing air. These samples were named as SiO_2@SnO_2-200-*m*, where *m* represents the Sn/Si molar ratio used in the preparation process. SiO_2@SnO_2 microspheres with sizes of 500 and 700 nm were also prepared and named according to above method. Respective amounts of 0.85 and 0.65 g of $Na_2SnO_3{\cdot}4H_2O$ with Sn/Si molar ratio of 0.3 and 0.23 were used to prepare SiO_2@SnO_2 microspheres with sizes of 500 and 700 nm to obtain microspheres with similar SnO_2 shell thickness to that of SiO_2@SnO_2-200−0.5.

SnO_2 hollow microspheres were prepared by etching the SiO_2 core of SiO_2@SnO_2 microspheres with NaOH solution with a concentration of 2 mol·L^{-1} at 80 °C for 1 h. Then the SnO_2 hollow microspheres were dried in an oven at 80 °C for 12 h after several cycles of centrifugation and redispersion in water. The obtained SnO_2 hollow microspheres were named according to the name of SiO_2@SnO_2 microspheres used in the preparation process. For example, SnO_2-200-1 means it was prepared from SiO_2@SnO_2-200-1. The entire process is shown in Scheme 1.

2.3. Characterization. Powder X-ray diffraction patterns of the microsphere samples were conducted on a Rigaku D/max-Ultima III X-ray powder diffractometer, operated at a 45 kV and 40 mA, with a scan speed of 10°·min^{-1} and a scan range between 20° and 80°, using Ni-filtered Cu Kα radiation, λ = 0.15406 nm. The morphology of the microspheres was investigated by using a scanning electron microscope (SEM; Zeiss Supra 55) with an accelerating voltage of 20 kV. Transmission electron microscopy (TEM) images were recorded on a Hitachi H-800 transmission electron microscope

DOI: 10.1021/acs.iecr.6b00060
Ind. Eng. Chem. Res. 2016, 55, 3588−3595

operated at 100 kV. High resolution transmission electron microscopy (HRTEM) images were noted on JEOL JEM-2010 microscope with an accelerating voltage of 200 kV. The specific surface area, pore volume, and size analysis were measured through Brunauer−Emmett−Teller (BET) and Barrett−Joyner−Halenda (BJH) methods, respectively, on a Micromeritics Surface Area & Porosity Gemini VII 2390 system. All the samples were degassed at 200 °C for 8 h prior to the measurements.

2.4. Measurements of Gas Sensing Performance. The fabrication process of the sensors based on SnO_2 hollow microspheres is similar to that reported elsewhere.[22] Proper amounts of SnO_2 hollow microspheres were slightly ground together with several drops of ethanol in an agate mortar to form a slurry, and the slurry was coated on a ceramic tube with a diameter of 1.2 mm and length of 4 mm, being positioned with a pair of Au electrodes and four Pt wires on both ends of the tube. A Ni−Cr heating wire through the tube was employed as a heater to control the operating temperature by tuning the heating current. The gas sensors were aged at 200 °C for 4 days before the gas sensing measurement. Gas sensing tests were performed on a CGS-8 intelligent gas sensing analysis system (Elite Tech Co., Ltd.) at a relative humidity of 25−45%. A schematic diagram of analysis system and experimental process were illustrated in the previous report.[23] The gas response of the sensor was defined as R_g/R_a for oxidizing gas and R_a/R_g for reducing gas, where R_a and R_g were the resistances of the sensor in air and test gas. The response and recovery time is defined as the time taken when the response value reaches 90% of the final equilibrium one.

3. RESULTS AND DISCUSSION

3.1. Structure and Morphology of SnO_2 Hollow Microspheres. Figure 1 shows the XRD patterns of SiO_2-200, uncalcinated SiO_2@SnO_2-200-0.5, calcinated SiO_2@SnO_2-200-0.5, and SnO_2-200-0.5, respectively. The XRD pattern of SiO_2 microspheres (Figure 1a) indicates an amorphous phase of the SiO_2 (JCPDS card 82-0512). After coating with SnO_2, the reflection due to the SnO_2 phase can be observed in addition to SiO_2 in the pattern of uncalcinated SiO_2@SnO_2 microspheres. The broad diffraction peaks of the SnO_2 layer are weak because the layer is incompletely crystallized during the coating process (Figure 1b). The intensity of SnO_2 diffraction peaks increases slightly after calcination at 400 °C (Figure 1c), indicating the crystallinity of SnO_2 was improved slightly. The characteristic peak of SiO_2 disappears in the XRD pattern of SnO_2 hollow spheres (Figure 1d), and no other diffraction peaks can be observed in the pattern, manifesting that the SiO_2 microsphere templates were completely removed by etching with NaOH solution. Besides, all diffraction peaks of SnO_2 hollow spheres can be indexed to the tetragonal rutile structure of SnO_2 (JCPDS card 77-0450). The crystalline size of SnO_2 hollow microspheres calculated by the Scherrer equation based on the full-width at half-maximum of the (110) diffraction peak is about 3.5 nm.

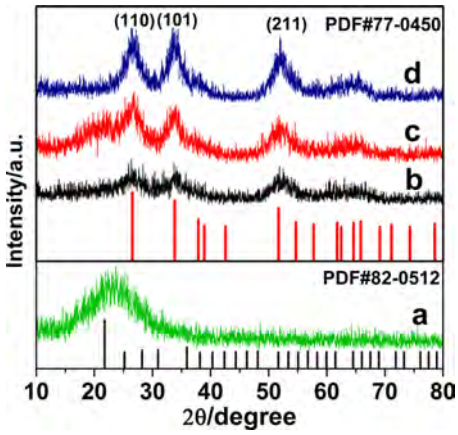

Figure 1. XRD patterns of (a) SiO_2-200, (b) uncalcinated SiO_2@SnO_2-200-0.5, (c) calcinated SiO_2@SnO_2-200-0.5, and (d) SnO_2-200-0.5.

The typical morphologies of the templates were observed by SEM, and the results are displayed in Figure 2. The as-prepared SiO_2 microspheres with smooth surface are relatively uniform and monodisperse (see part a, b, and c in Figure 2). Hence the prepared SiO_2 microspheres are ideal templates to prepare uniform hollow microspheres. The size of the SiO_2 microspheres template can be easily tuned by adjusting the amount of deionized water and TEOS, and the SEM images show that SiO_2 microspheres have a mean diameter of about 200, 500, and 700 nm, respectively. SiO_2@SnO_2 with core−shell structure was obtained after coating SnO_2 on the surface of SiO_2 microsphere and annealing at 400 °C. As shown in Figure 2 panels d−f, the surface of SiO_2 microsphere becomes rough, indicating that SnO_2 particles were successfully loaded on the surface of SiO_2. After etching by NaOH solution, the cores of SiO_2@SnO_2 microspheres were removed, and give rise to SnO_2 hollow microspheres which can be clearly seen in Figure 2g−i. The size of the hollow microspheres can be easily controlled by using different-sized templates, and the thickness of shell can be tuned by controlling the loading amount of SnO_2. In addition, SnO_2 hollow microspheres have uniform size due to the monodispersed SiO_2 templates.

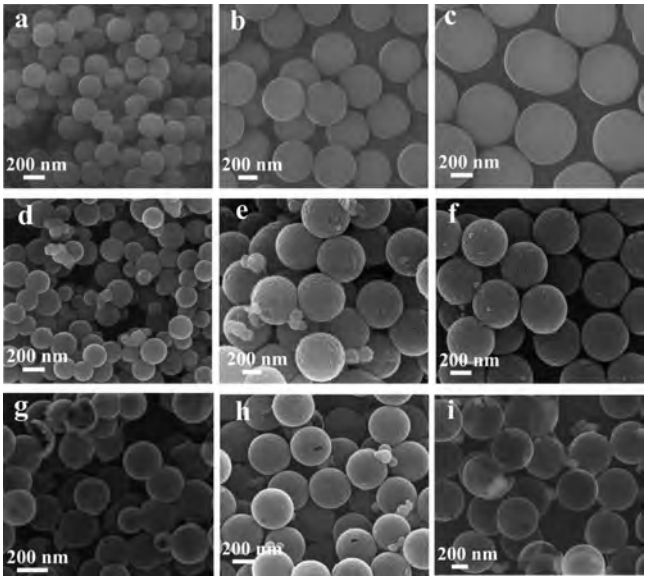

Figure 2. SEM images of (a) SiO_2-200, (b) SiO_2-500, (c) SiO_2-700, (d) SiO_2@SnO_2-200, (e) SiO_2@SnO_2-500, (f) SiO_2@SnO_2-700, (g) SnO_2-200, (h) SnO_2-500, and (i) SnO_2-700.

The SnO_2 hollow microspheres were further characterized by TEM, and the results indicate the hollow nature of the SnO_2 microspheres. As shown in Figure 3, all samples have a regular hollow spherical structure after removing the SiO_2 microsphere

DOI: 10.1021/acs.iecr.6b00060
Ind. Eng. Chem. Res. 2016, 55, 3588−3595

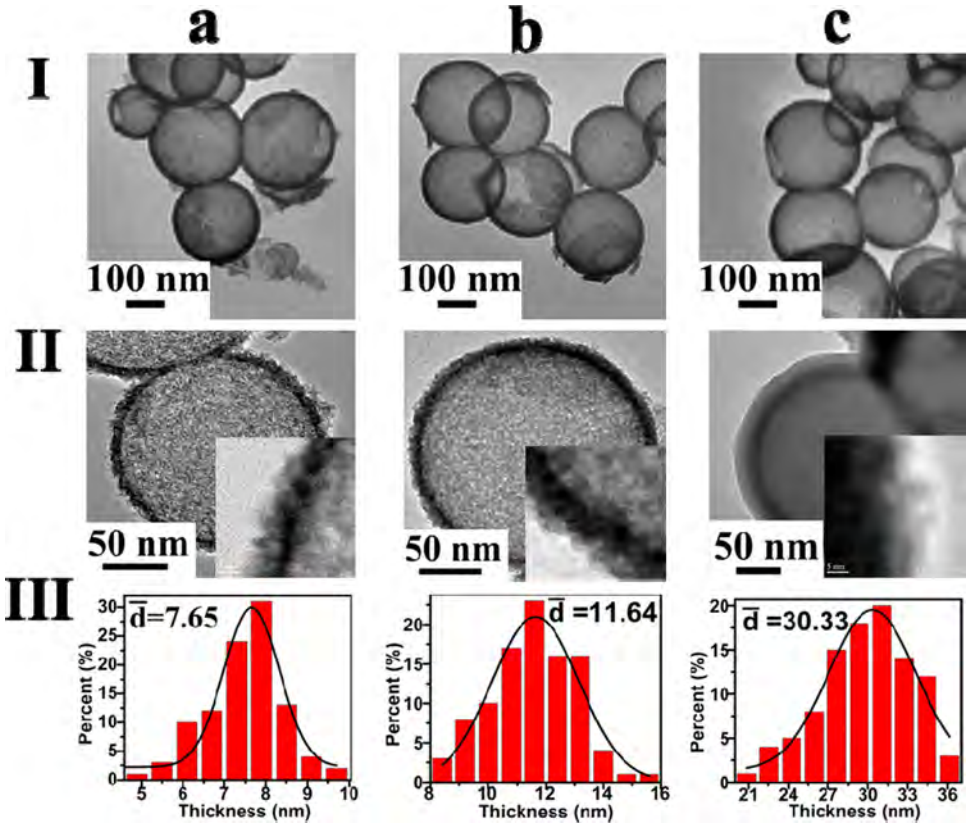

Figure 3. TEM images (I), HRTEM images (II), and shell thickness distribution (III) of (a) SnO_2-200-0.5, (b) SnO_2-200-1 and (c) SnO_2-200-1.5.

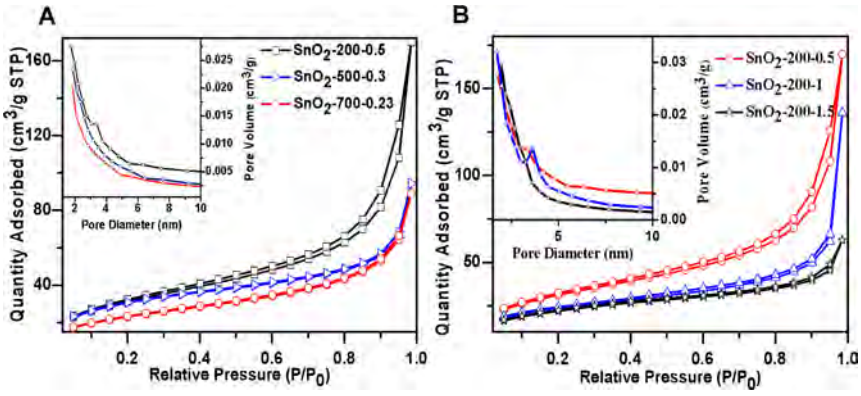

Figure 4. Nitrogen adsorption−desorption isotherms and pore size distribution (inset) of SnO_2 hollow microspheres with different sizes (A) and different shell thickness (B).

cores. The shell thickness of all products is uniform, indicating the homogeneous loading of SnO_2 on the surface of SiO_2 microspheres. The shell thickness, which can be facilely tuned by controlling the loading amount of SnO_2, increased from 7.65 to 30.33 nm as the molar ratio of Na_2SnO_3 to SiO_2 increased from 0.5 to 1.5. The HRTEM images suggest that the SnO_2 hollow microspheres are composed of interconnected nanocrystallites (Figure 3B). Moreover, the crystallite size of the SnO_2 hollow microsphere increases as the SnO_2 loading amount increases. The crystallite size of SnO_2-200-1.5 (5.64 nm) is 2-fold larger than the size of SnO_2-200-0.5 (2.81 nm). These results suggest that the loading amount of SnO_2 not only has significant impact on the shell thickness but also exerts considerable influence on the crystallite size of SnO_2 hollow microspheres. It should be noted that it is difficult to form hollow microspheres when the Sn/Si molar ratio was decreased to 0.25. The SEM and TEM images of SnO_2-200-0.25 are displayed in Figure S1 in the Supporting Information.

The specific surface area and pore-size distribution are two key factors for the gas sensing materials in sensor application; therefore, the specific surface area and porosity property of the SnO_2 hollow microspheres were characterized by nitrogen adsorption and desorption method. Figure 4 shows the N_2 adsorption−desorption isotherms and the corresponding pore-size distribution curves of all samples. In all cases, typical III isotherm with H3-type hysteresis loops ($P/P_0 > 0.5$) are observed, indicating the presence of mesopores in all samples. This type of hysteresis loops does not exhibit any limiting adsorption at the high P/P_0 region, which is commonly attributed to particle aggregates with slit-shaped pores.

DOI: 10.1021/acs.iecr.6b00060
Ind. Eng. Chem. Res. 2016, 55, 3588−3595

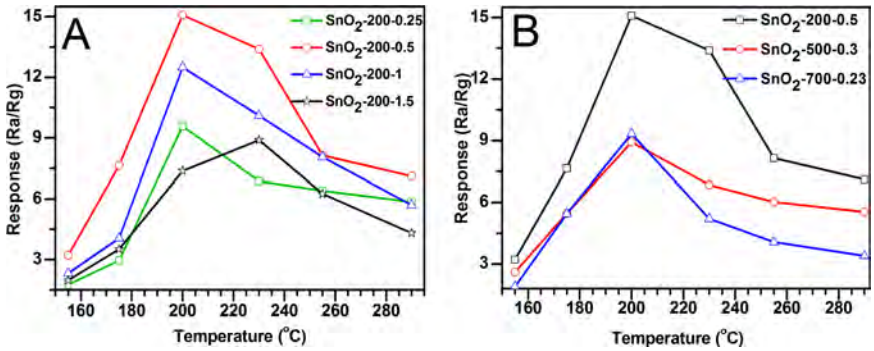

Figure 5. Response of SnO_2 hollow microspheres to 50 ppm acetone at different operating temperature.

Interestingly, the pore size of the SnO_2 hollow microspheres increases markedly with the decrease of the diameter of the sphere and the amount of Na_2SnO_3 (inset in Figure 4). Typically, the hollow microspheres give a complete mesopore distribution in the range of 4.28−6.66 nm, and the average pore diameter of SnO_2-200-0.5 reaches 6.66 nm, which is the largest among these samples. Moreover, SnO_2-200-0.5 possesses the maximum specific surface area (122.65 $m^2 \cdot g^{-1}$), which is much larger than that of SnO_2-500-0.3 (103.59 $m^2 \cdot g^{-1}$), SnO_2-700-0.23 (92.56 $m^2 \cdot g^{-1}$), SnO_2-200-1 (110.02 $m^2 \cdot g^{-1}$) and SnO_2-200-1.5 (81.30 $m^2 \cdot g^{-1}$).

It is well-known that the response of resistive sensors is considerably affected by the operating temperature. To obtain the optimal operating temperature, the sensing responses of sensors are recorded at operating temperatures of 155, 175, 200, 230, 255, and 290 °C with 50 ppm acetone, and the results are shown in Figure 5A. It can be seen that the response increases first and then decreases when the operating temperature increases from 155 to 290 °C. It is obvious that SnO_2-200-0.5 has the highest response to acetone among the investigated samples, and the response reaches the highest value of 15 at 200 °C. Therefore, the optimal operating temperature for SnO_2-200-0.5 is 200 °C. The gas sensing response is related to the adsorption, desorption, and reaction of the target gas on the surface of sensing material. SnO_2-200-0.5 has a higher specific surface area, resulting in more active sites on the surface for physical or chemical absorption of gases and increasing the reaction opportunity between gas molecules and gas sensing materials. In addition, the wider pore diameter can facilitate the diffusion of gas onto the surface of materials, and the smaller crystallite size is also beneficial to the gas sensing response. Although SnO_2-200-0.25 has a larger specific surface area and smaller crystal size than SnO_2-200-0.5 and SnO_2-200-1, its sensing sensitivity toward acetone is considerably lower than SnO_2-200-0.5 and SnO_2-200-1, indicating that the hollow structure is vital for improving the sensing sensitivity of SnO_2 material. The sensing response of SnO_2 hollow microspheres with different diameters are illustrated in Figure 5B. It can be seen that the response decreases with the increase of the diameter because the surface/volume ratio decreases when the diameter becomes larger (the shell thickness of SnO_2-500-0.3 and SnO_2-700-0.23 is 10.52 and 7.86 nm, respectively), reducing the adsorption and reaction chances of gases on the surface of SnO_2.

The sensing mechanism of the SnO_2 hollow spheres to acetone is based on the surface conduction modulation by the adsorption and desorption of gas molecules on the surface of materials. Oxygen molecules are adsorbed on the surface of SnO_2 nanoparticles, and the adsorbed oxygen species (O_2^-, O^-, and O^{2-}) are generated by acquiring electrons from the conduction band when SnO_2 hollow spheres are heated in air, as represented in eq 1, 2, 3, and 4.[24,25] Upon exposure to acetone, acetone gas molecules can react with the adsorbed oxygen species on the outer and inner surface of SnO_2 hollow spheres, and CH_3C^+O, CH_3O^-, C^+H_3, CO, and CO_2 are formed, as shown in eq 5, 6 and 7.[26] Acetone molecules donate electrons to the previously adsorbed oxygen species. Thus, electrons are released into the conduction band of the materials, thereby reducing the resistance of SnO_2 hollow spheres. The sensing mechanism of SnO_2 hollow spheres to acetone is illustrated in Scheme 2.

$$O_2(gas) \rightarrow O_2(ads) \quad (1)$$

$$O_2(ads) + e^- \rightarrow O_2^-(ads) \quad (2)$$

$$O_2^-(ads) + e^- \rightarrow 2O^-(ads) \quad (3)$$

$$O^-(ads) + e^- \rightarrow O^{2-}(ads) \quad (4)$$

$$CH_3COCH_3(gas) + O^- \rightarrow CH_3C^+O + CH_3O^- + e^- \quad (5)$$

$$CH_3C^+O \rightarrow C^+H_3 + CO \quad (6)$$

$$CO + O^- \rightarrow CO_2 + e^- \quad (7)$$

Another issue we would like to emphasize is the selectivity of SnO_2-200-0.5. It has been reported that gas sensors based on semiconductor metal oxides are often sensitive to several gas species simultaneously, which is adverse for their practical

Scheme 2. Schematic Diagram of Acetone Sensing Mechanism of SnO_2 Hollow Spheres

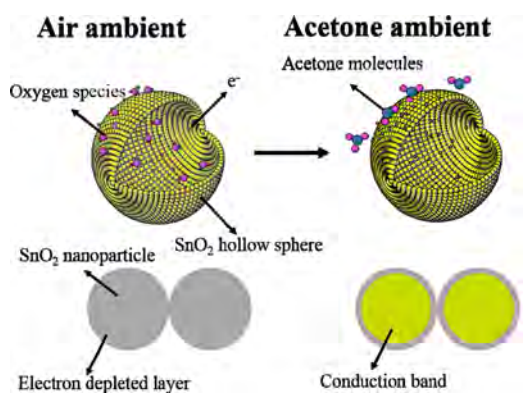

DOI: 10.1021/acs.iecr.6b00060
Ind. Eng. Chem. Res. 2016, 55, 3588−3595

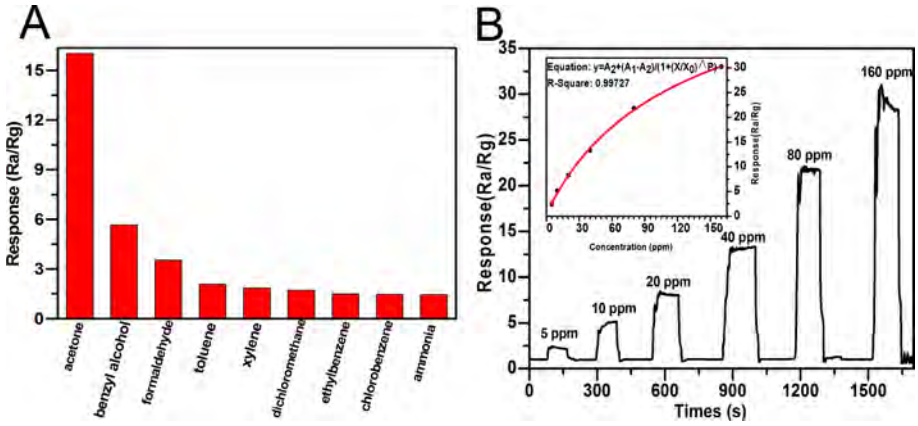

Figure 6. (A) Response of SnO_2-200-0.5 to various gases with concentration of 50 ppm at 200 °C; (B) response curve and linear fitting curve of the sensing response of SnO_2-200-0.5 to acetone with different concentration at 200 °C.

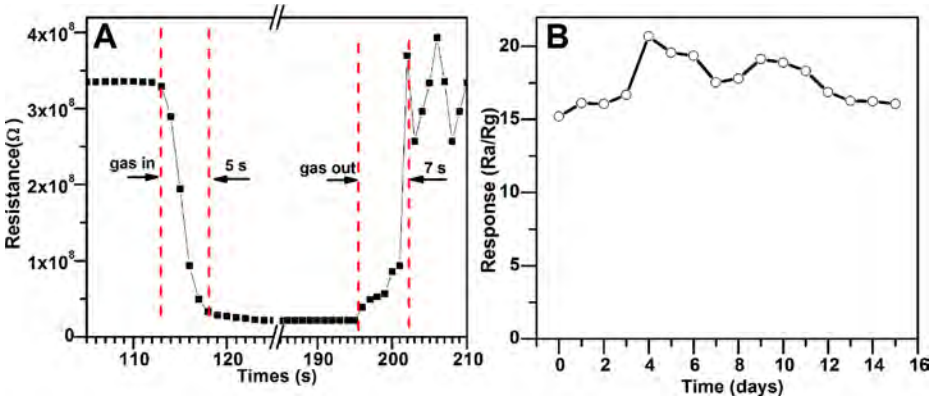

Figure 7. (A) Response and recovery times, and (B) response stability of SnO_2-200-0.5 toward 50 ppm acetone at 200 °C.

applications. Figure 6A shows the gas sensing response of SnO_2-200−0.5 to different gases with concentration of 50 ppm at 200 °C. Obviously, the response toward acetone is much higher than that toward benzyl alcohol, formaldehyde, toluene, xylene, ethylbenzene, dichloromethane, chlorobenzene, and ammonia. SnO_2-200-0.5 exhibits a maximum response to acetone with a value of 15, while for others gases, the responses do not exceed 6. It is well-known that the sensing response is associated with the adsorption and reaction of gas molecules on the sensing materials. On one hand, the polar nature of the surface of the SnO_2 hollow sphere will facilitate the adsorption of polar molecules. Hence, acetone, benzyl alcohol, formaldehyde, dichloromethane, ammonia, and chlorobenzene are much easier to be adsorbed on the surface of SnO_2 than toluene, xylene, and ethylbenzene. On the other hand, the bond dissociation energy of CH_3-COCH_3 (352 kJ·mol^{-1}) is smaller than that of $HO-CH_2C_6H_5$ (366 kJ·mol^{-1}), H−COH (368 kJ·mol^{-1}), $H-CH_2C_6H_4CH_3$ (367 kJ·mol^{-1}), $H-CH_2C_6H_5$ (371 kJ·mol^{-1}), $H-CHCl_2$ (407 kJ·mol^{-1}), $H-NH_2$ (452 kJ·mol^{-1}), and $H-C_6H_5$ (472 kJ·mol^{-1}), suggesting that acetone is easier to react with the adsorbed oxygen species than other gas molecules. Therefore, more acetone molecules can react with the adsorbed oxygen species and can release more electrons than other gas molecules. As a result, the SnO_2 hollow microsphere has good sensing response and selectivity to acetone.

The sensing responses of SnO_2-200-0.5 to acetone with a concentration of 5, 10, 20, 40, 80, and 160 ppm were tested in sequence at the optimal operating temperature of 200 °C, and the obtained results are shown in Figure 6B. It can be observed that the sensing response increases nearly linearly when the concentration of acetone increases from 5 to 160 ppm. The sensing response toward 5 ppm acetone reaches 2.4, indicating that SnO_2-200-0.5 can be potentially used as sensing material for detecting acetone at low concentration. The response and recovery times are another key factor for gas sensors. Figure 7A shows that the response and recovery times of SnO_2-200-0.5 toward 50 ppm acetone in air atmosphere are about 5 and 7 s as marked in the graph, respectively. It should be noted that SnO_2-200-0.5 showed a relatively high resistance of 360 MΩ because of its hollow structure and small crystallite size which benefits the formation of an electron depletion layer in the whole nanocrystallite, favoring the improvement of a sensing response. The response stability of the sensor is very important for its practical applications. It can be seen that SnO_2-200-0.5 maintains high sensing response (larger than 15) to 50 ppm acetone during the sensing stability test (Figure 7B), indicating SnO_2-200-0.5 is expected to have good long-term stability, which benefits its practical application. In comparison with SnO_2-based sensors reported previously, both response and recovery times are much shorter than most of the reported times as summarized in Table 1. Therefore, SnO_2-200-0.5 shows excellent gas sensing performance, such as lower optimal operating temperature, higher sensing response, and faster response and recovery.

DOI: 10.1021/acs.iecr.6b00060
Ind. Eng. Chem. Res. 2016, 55, 3588−3595

Table 1. Sensing Performance of SnO_2 Materials to Acetone Reported and in This Work

materials	(ppm)	temp (°C)	response	response and recovery time (s)	ref
SnO_2 nanotube	20	350	6.4	10/9	12
SnO_2 nanoparticles	200	240	28.2	−/−	27
SnO_2 nanomaterial	100	250	18.5	4.3/156.3	28
Aurelia-like SnO_2	10	240	4.7	2/23	29
Hollow SnO_2 nanobelts	5	260	5.7	38/9	30
Square-shaped SnO_2 nanowires	20	290	5.5	7/10	15
SnO_2 nano polyhedrons	200	370	48	9.7/5.8	14
Ce-doped SnO_2 hollow spheres	100	250	11.9	18/7	20
Hierarchical α-Fe_2O_3/SnO_2 composites	100	250	16.8	3/90	31
SnO_2 hollow spheres	50	200	16	5/7	this work

4. CONCLUSIONS

SnO_2 hollow microspheres were prepared through a simple method by using SiO_2 microspheres as a template and Na_2SnO_3 as a tin source. The diameter of the SnO_2 hollow microspheres can be easily tuned from 200 to 700 nm by using SiO_2 microspheres with size from 200 to 700 nm, and the shell thickness of the hollow microspheres can be adjusted in the range of 7−33 nm by controlling the deposition amount of Na_2SnO_3. Gas sensors fabricated from the as-prepared SnO_2 hollow microspheres exhibited excellent acetone sensing performance. Acetone sensing tests showed that the sensing response of SnO_2 hollow microspheres to acetone increases with the decrease of the diameter, the shell thickness, and the crystal size of SnO_2 hollow microspheres, because the small diameter and thin thickness of microspheres facilitate the diffusion of gases, and the small crystal size of SnO_2 benefits the adsorption and reaction of gases on the surface of SnO_2. Besides, SnO_2 hollow microspheres also possess the advantages of low operating temperature, high sensing selectivity, fast response and recovery, and good stability. Therefore, such SnO_2 hollow microspheres would have potential applications in the fields of sensors.

■ ASSOCIATED CONTENT

Supporting Information

The Supporting Information is available free of charge on the ACS Publications website at DOI: 10.1021/acs.iecr.6b00060.

SEM, TEM, HRTEM, crystal size distribution, Nitrogen adsorption−desorption isotherms and pore size distribution of SnO_2-200-0.25 (PDF)

■ AUTHOR INFORMATION

Corresponding Authors

*Fax and Tel: + 86-10-64436992. E-mail: tangpg@mail.buct.edu.cn.

*E-mail: lidq@mail.buct.edu.cn.

Notes

The authors declare no competing financial interest.

■ ACKNOWLEDGMENTS

This work was supported by the National Natural Science Foundations of China (21371022, U1507119), the 973 Project (2011CBA00508), and the Fundamental Research Funds for the Central Universities (YS1406).

■ REFERENCES

(1) Singkammo, S.; Wisitsoraat, A.; Sriprachuabwong, C.; Tuantranont, A.; Phanichphant, S.; Liewhiran, C. Electrolytically exfoliated graphene-loaded flame-made Ni-doped SnO_2 composite film for acetone sensing. *ACS Appl. Mater. Interfaces* **2015**, *7*, 3077.

(2) Yamazoe, N. New approaches for improving semiconductor gas sensors. *Sens. Actuators, B* **1991**, *5*, 7.

(3) Zhang, H.; Wu, R.; Chen, Z.; Liu, G.; Zhang, Z.; Jiao, Z. Self-assembly fabrication of 3D flower-like ZnO hierarchical nanostructures and their gas sensing properties. *CrystEngComm* **2012**, *14*, 1775.

(4) Manjula, P.; Boppella, R.; Manorama, S. V. A facile and green approach for the controlled synthesis of porous SnO_2 nanospheres: Application as an efficient photocatalyst and an excellent gas sensing material. *ACS Appl. Mater. Interfaces* **2012**, *4*, 6252.

(5) Lu, R.; Zhou, W.; Shi, K.; Yang, Y.; Wang, L.; Pan, K.; Tian, C.; Ren, Z.; Fu, H. Alumina decorated TiO_2 nanotubes with ordered mesoporous walls as high sensitivity NOx gas sensors at room temperature. *Nanoscale* **2013**, *5*, 8569.

(6) Wang, L.; Deng, J.; Lou, Z.; Zhang, T. Cross-linked p-type Co_3O_4 octahedral nanoparticles in 1D n-type TiO_2 nanofibers for high-performance sensing devices. *J. Mater. Chem. A* **2014**, *2*, 10022.

(7) Elouali, S.; Bloor, L. G.; Binions, R.; Parkin, I. P.; Carmalt, C. J.; Darr, J. A. Gas sensing with nano-indium oxides (In_2O_3) prepared via continuous hydrothermal flow synthesis. *Langmuir* **2012**, *28*, 1879.

(8) Wang, L.; Fei, T.; Lou, Z.; Zhang, T. Three-dimensional hierarchical flowerlike α-Fe_2O_3 nanostructures: synthesis and ethanol-sensing properties. *ACS Appl. Mater. Interfaces* **2011**, *3*, 4689.

(9) Stoycheva, T.; Annanouch, F. E.; Gràcia, I.; Llobet, E.; Blackman, C.; Correig, X.; Vallejos, S. Micromachined gas sensors based on tungsten oxide nanoneedles directly integrated via aerosol assisted CVD. *Sens. Actuators, B* **2014**, *198*, 210.

(10) Korotcenkov, G. Metal oxides for solid-state gas sensors: What determines our choice? *Mater. Sci. Eng., B* **2007**, *139*, 1.

(11) Barsan, N.; Schweizer-Berberich, M.; Göpel, W. Fundamental and practical aspects in the design of nanoscaled SnO_2 gas sensors: a status report. *Fresenius' J. Anal. Chem.* **1999**, *365*, 287.

(12) Zhu, S.; Zhang, D.; Gu, J.; Xu, J.; Dong, J.; Li, J. Biotemplate fabrication of SnO_2 nanotubular materials by a sonochemical method for gas sensors. *J. Nanopart. Res.* **2010**, *12*, 1389.

(13) Tian, S.; Gao, Y.; Zeng, D.; Xie, C. Effect of zinc doping on microstructures and gas-sensing properties of SnO_2 nanocrystals. *J. Am. Ceram. Soc.* **2012**, *95*, 436.

(14) Chen, D.; Xu, J.; Xie, Z.; Shen, G. Nanowires assembled SnO_2 nanopolyhedrons with enhanced gas sensing properties. *ACS Appl. Mater. Interfaces* **2011**, *3*, 2112.

(15) Qin, L.; Xu, J.; Dong, X.; Pan, Q.; Cheng, Z.; Xiang, Q.; Li, F. The template-free synthesis of square-shaped SnO_2 nanowires: the temperature effect and acetone gas sensors. *Nanotechnology* **2008**, *19*, 185705.

(16) Lee, J.-H. Gas sensors using hierarchical and hollow oxide nanostructures: overview. *Sens. Actuators, B* **2009**, *140*, 319.

(17) Caihong, W.; Chu, X.; Wu, M. Highly sensitive gas sensors based on hollow SnO_2 spheres prepared by carbon sphere template method. *Sens. Actuators, B* **2007**, *120*, 508.

(18) Tan, Y.; Li, C.; Wang, Y.; Tang, J.; Ouyang, X. Fast-response and high sensitivity gas sensors based on SnO_2 hollow spheres. *Thin Solid Films* **2008**, *516*, 7840.

(19) Wang, H.; Liang, J.; Fan, H.; Xi, B.; Zhang, M.; Xiong, S.; Zhu, Y.; Qian, Y. Synthesis and gas sensitivities of SnO_2 nanorods and hollow microspheres. *J. Solid State Chem.* **2008**, *181*, 122.

DOI: 10.1021/acs.iecr.6b00060
Ind. Eng. Chem. Res. 2016, 55, 3588−3595

(20) Song, P.; Wang, Q.; Yang, Z. Preparation, characterization and acetone sensing properties of Ce-doped SnO_2 hollow spheres. *Sens. Actuators, B* **2012**, *173*, 839.
(21) Hsu, W. P.; Yu, R.; Matijević, E. Paper whiteners: I. titania coated silica. *J. Colloid Interface Sci.* **1993**, *156*, 56.
(22) Liu, L.; Li, S.; Zhuang, J.; Wang, L.; Zhang, J.; Li, H.; Liu, Z.; Han, Y.; Jiang, X.; Zhang, P. Improved selective acetone sensing properties of Co-doped ZnO nanofibers by electrospinning. *Sens. Actuators, B* **2011**, *155*, 782.
(23) Qi, Q.; Zhao, J.; Xuan, R.-F.; Wang, P.-P.; Feng, L.-L.; Zhou, L.-J.; Wang, D.-J.; Li, G.-D. Sensitive ethanol sensors fabricated from p-type $La_{0.7}Sr_{0.3}FeO_3$ nanoparticles and n-type SnO_2 nanofibers. *Sens. Actuators, B* **2014**, *191*, 659.
(24) Rai, P.; Khan, R.; Ahmad, R.; Hahn, Y.-B.; Lee, I.-H.; Yu, Y.-T. Gas sensing properties of single crystalline ZnO nanowires grown by thermal evaporation technique. *Curr. Appl. Phys.* **2013**, *13*, 1769.
(25) Patil, G. E.; Kajale, D. D.; Chavan, D. N.; Pawar, N. K.; Ahire, P. T.; Shinde, S. D.; Gaikwad, V. B.; Jain, G. H. Synthesis, characterization and gas sensing performance of SnO_2 thin films prepared by spray pyrolysis. *Bull. Mater. Sci.* **2011**, *34*, 1.
(26) Chang, S.-J.; Hsueh, T.-J.; Chen, I.; Hsieh, S.-F.; Chang, S.-P.; Hsu, C.-L.; Lin, Y.-R.; Huang, B.-R. Highly sensitive ZnO nanowire acetone vapor sensor with Au adsorption. *IEEE T. Nanotechnol.* **2008**, *7*, 754.
(27) Li, L.; Lin, H.; Qu, F. Synthesis of mesoporous SnO_2 nanomaterials with selective gas-sensing properties. *J. Sol-Gel Sci. Technol.* **2013**, *67*, 545.
(28) Tan, W.; Ruan, X.; Yu, Q.; Yu, Z.; Huang, X. Fabrication of a SnO_2-based acetone gas sensor enhanced by molecular imprinting. *Sensors* **2015**, *15*, 352.
(29) Yu, H.; Wang, S.; Xiao, C.; Xiao, B.; Wang, P.; Li, Z.; Zhang, M. Enhanced acetone gas sensing properties by aurelia-like SnO_2 micro-nanostructures. *CrystEngComm* **2015**, *17*, 4316.
(30) Li, W.; Ma, S.; Luo, J.; Mao, Y.; Cheng, L.; Gengzang, D.; Xu, X.; Yan, S. Synthesis of hollow SnO_2 nanobelts and their application in acetone sensor. *Mater. Lett.* **2014**, *132*, 338.
(31) Sun, P.; Cai, Y.; Du, S.; Xu, X.; You, L.; Ma, J.; Liu, F.; Liang, X.; Sun, Y.; Lu, G. Hierarchical α-Fe_2O_3/SnO_2 semiconductor composites: Hydrothermal synthesis and gas sensing properties. *Sens. Actuators, B* **2013**, *182*, 336.

DOI: 10.1021/acs.iecr.6b00060
Ind. Eng. Chem. Res. 2016, 55, 3588−3595